# 7A.6 NUMERICAL SIMULATIONS OF INTERACTIONS BETWEEN SQUALL LINES AND SUPERCELLS

Adam J. French* and Matthew D. Parker
North Carolina State University, Raleigh, North Carolina

## 1. INTRODUCTION

A considerable fraction of significant severe weather (damaging winds, large hail and/or tornadoes) tends to occur with organized convection in the form of quasi-linear convective systems (QLCSs or "squall lines") and supercell thunderstorms. Given the apparent threat posed by these systems, it is no surprise that they have each received a great deal of attention in the severe storms literature over the years, leading to an improved of understanding of both phenomena. However, these two convective modes are often studied in isolation, with a given study focusing on one mode or the other, despite the fact that they often occur in close proximity to one another (e.g. French and Parker 2008). This has left a gap in the knowledge base regarding how supercells and squall lines interact when they are present in close proximity to one another, and what these interactions might mean for the production of severe weather. The present paper looks to address part of this question, with an investigation of how isolated supercell thunderstorms merge with squall lines.

## 2. BACKGROUND

Past literature dealing with squall line-supercell mergers has generally focused on observation-based analysis of individual cases, many of which produced significant tornadoes. Goodman and Knupp (1993) investigated a case from November 1989 wherein a merger between a squall line and isolated supercell coincided with the development of an F4 tornado that struck Huntsville, AL. Using WSR-88D radar data, observations from a nearby surface mesonet, and visual observations of the storm, the authors demonstrated that tornadogenesis appeared to coincide with an interaction between the supercell and the gust front associated with the squall line's cold pool. Furthermore, these observations also showed a "distortion" of the squall line's gust front, resulting from the merger. As the squall line approached the supercell, forward progress of its gust front slowed in the vicinity of the merger and accelerated south of the merger location, effectively appearing to "wrap around" the supercell's mesocyclone. This indicates that the supercell effectively altered the structure of the squall line during the merger process. Additional studies also suggest a propensity for the supercell to play a dominant role in the merger process. Wolf (1998) analyzed what he described as the "unexpected evolution" of a merger between a supercell and bow that produced a large high-precipitation supercell, and continued to produce tornadoes for over an hour after the merger. Similar results were seen by Sabones et al. (1996) and Wolf et al. (1996), both of which documented interactions between squall lines or bowing line segments and supercells coinciding with tornadogenesis.

These past studies suggest that squall line supercell mergers tend to favor continued maintenance of supercell structures, and may be a trigger for tornadogenesis. However, this may not always be the case. Knupp et al. (2003) and Lindsey and Bunkers (2005) both detail cases where cell mergers appear to be detrimental to sustained supercell organization, and Bunkers et al. (2006) list "supercell merges or interacts with other thunderstorms which can either destroy its circulation or cause it to evolve into another convective mode" as an avenue for supercell demise. In addition, as pointed out by Wolf (1998), the concept that the supercell remains the dominant convective mode following an interaction with a squall line is not necessarily intuitive, as one might expect the strong outflow from the squall line to undercut the supercell and effectively remove its source of unstable inflowing air. In light of these questions, French and Parker (2009) undertook a study to examine a larger number of squall line-supercell merger cases in order to determine more general characteristics of these merger events. They found, as did the authors cited in the previous paragraph, that in the

**Corresponding author address:* Adam J. French, Department of Marine, Earth, & Atmospheric Sciences, North Carolina State University, Campus Box 8208, Raleigh, NC 27695–8208. E-mail: ajfrench@ncsu.edu

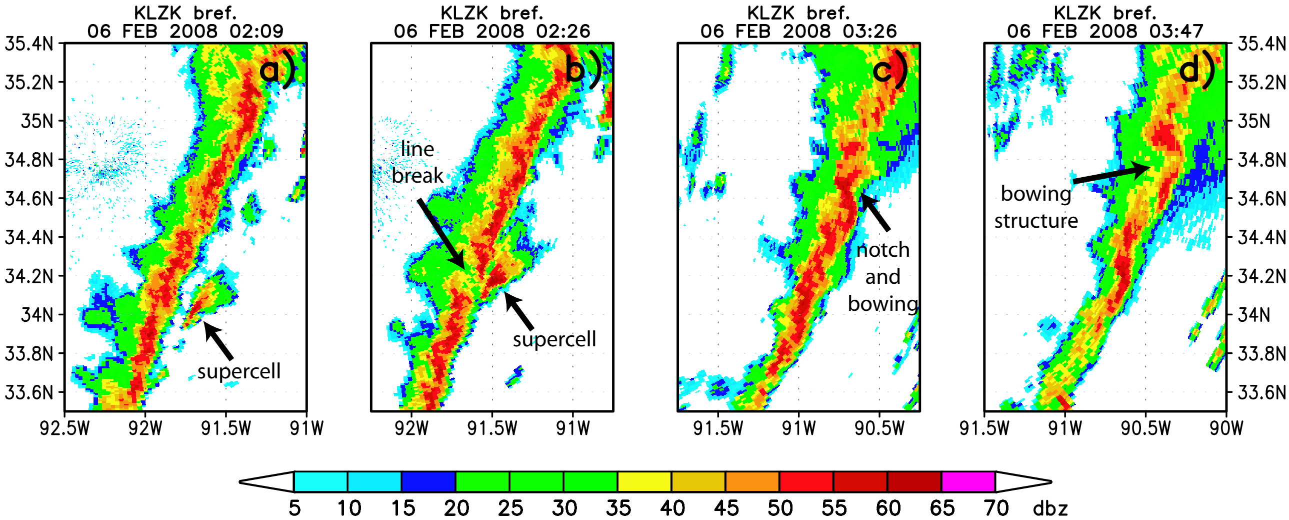


Figure 1: Base reflectivity from KLZK WSR-88D at (a) 0209 (b) 0226 (c) 0326 and (d) 0347 UTC 6 February 2008, illustrating some of the radar reflectivity structures commonly observed with merger events.

majority of their 8 cases (and in several additional cases analyzed since) that the supercell plays a dominate role in these types of merger events, remaining evident for 1-2 hours after the merger and fundamentally altering the structure of the squall line. Specifically, as illustrated in Fig. 1, the merger is generally preceded by a break or weakening of the squall line, followed by a period during which the supercell is evident as notch in the leading edge of the line, and an eventual evolution toward a bow echo type structure associated with the remnant supercell. Additionally, the supercell's mesocyclone circulation generally remained trackable in radial velocity data for 1-2 hours after the merger (not shown).

In short, a combination of past case studies and more recent work by the present authors points to mergers between squall lines and supercells largely being dominated by the supercell. However, little is still known about the convective-scale details of these types of events. In particular, how does the supercell merge with the squall line without being undercut by the squall line's outflow? And once the merger occurs, how is the supercell's mesocyclone circulation maintained? To address these questions we have run numerical simulations of two of our observed merger cases using the Weather Research and Forecasting (WRF) model.

## 3. METHODS

Past work by French and Parker (2008) has demonstrated that mesoscale environmental heterogeneity and forcing along mesoscale boundaries such as drylines and cold fronts play a significant role in the development of sustenance of multiple convective modes in close proximity to one another. In light of this, we chose to utilize the WRF model, run in "real data" or case study mode for the present study. We used the Advanced Research WRF core (WRF-ARW) version 3.2 for to simulate two squall line-supercell merger cases: 5 May 1995 (hereafter "5 May"), and 24 May 2008 (hereafter "24 May"). Each case illustrates a slightly different behavior common to multiple observed cases, as will be discussed in the next section.

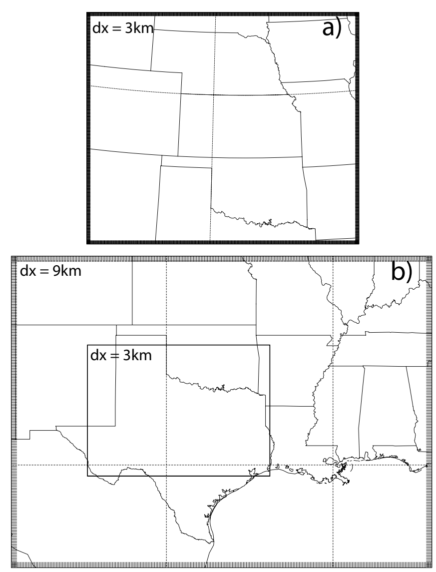


Figure 2: Model domains used for (a) the 24 May 2008 simulation and (b) the 5 May 1995 simulation. Horizontal grid spacing (in km) is provided in the upper left corner of each domain.

The 24 May case used a model domain of 1400 x 1200 km (x,y) (Fig. 2a) with a horizontal grid spac-

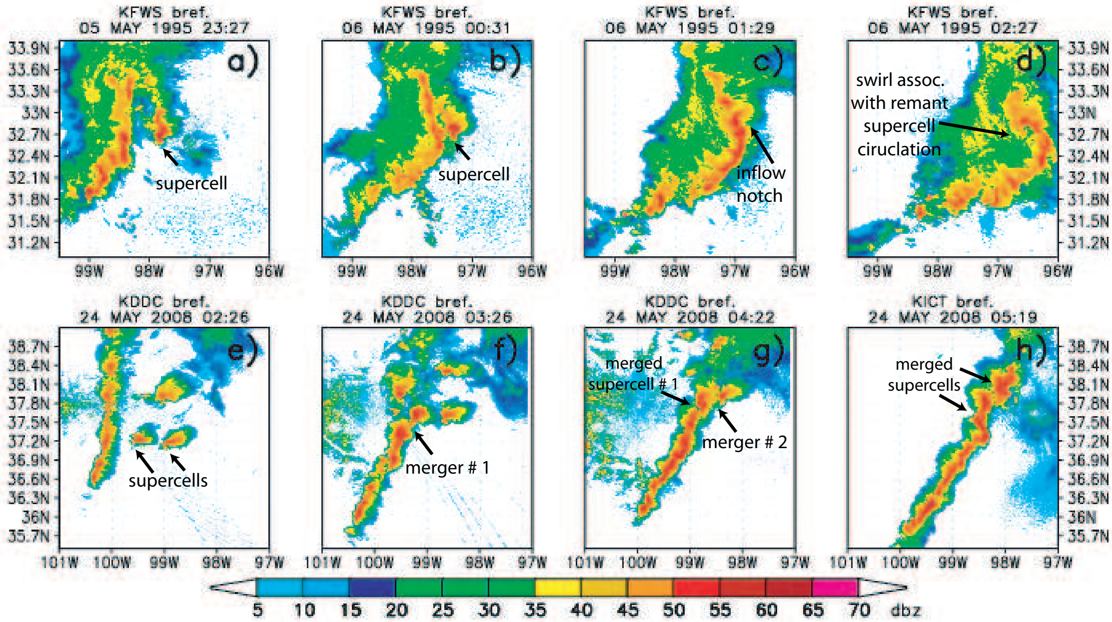


Figure 3: As in Fig. 1, but for KFWS WSR-88D at (a) 2327 UTC 5 May 1995, (b) 0031 (c) 0129 and (d) 0227 UTC 6 May 1995; KDDC WSR-88D at (e) 0226 (f) 0326 and (g) 0422 UTC 24 May 2008; and KICT WSR-88D at (h) 0519 UTC 24 May 2008.

ing of 3 km and initial and boundary conditions (updated every 6 hours) from the analysis fields of the NAM218 operational mesoscale forecast model (dx = 12 km). The 5 May simulation added an outer domain that was 2440 x 1800 km (x, y) with a horizontal grid spacing of 9 km (Fig. 2b). This was done because NAM218 data were not available for this case, and instead the coarser grid (32 km dx) North American Regional Reanalysis (NARR) data were used for initial and boundary conditions (updated every 3 hours). Both simulations used 50 vertical levels, with a vertical grid spacing that stretched from approximately 65 m near the surface to about 400 m at the model top of 16 km. Both simulations used the physical parameterizations summarized in table 1, with the only variation being that the 9 km domain in the 5 May simulation adds the Kain-Fritsch convective parameterization scheme.

## 4. OVERVIEW OF SIMULATIONS

### *4.1 5 May 1995 Case*

An overview of the convective evolution observed during the squall line-supercell merger on 5 May 1995 is provided in figure 3a-d. The event consisted of a merger between an isolated high precipitation supercell and a large bow echo. Following the merger, the supercell remained clearly evident as a localized circulation at the north end of the squall line, visible in both Doppler velocity and reflectivity data (e.g. Fig 3d). The bow echo also intensified following the merger with the bowing structure becoming more pronounced. This evolution, with the development of a strong bow echo and circulation at the north end of the squall line was a common occurrence in a number of observed cases. The background environmental conditions and evolution of the supercell in this case are discussed in detail by Calianese et al. (2002).

To simulate the 5 May 1995 case, the WRF model was run using a nested domain configuration centered on the southern plains of the United States (Fig. 2b) from an initial time of 1200 UTC on 5 May 1995, approximately 12 hours before the event. This provided sufficient time for small scale features not resolved in the initial conditions to develop from an otherwise "cold" start. Convection developed around 1900 UTC western Texas, with several cell mergers leading to the eventual organization of a squall line in west central Texas by 2300 UTC (not shown). An isolated high precipitation supercell began to develop just ahead of this squall line by approximately 2330 UTC (e.g. Fig. 4a), and proceeded to merge with the line approximately an hour later (Fig. 4b). Following the merger, several reflectivity patterns consistent with those seen in the actual 5 May 1995 case case were observed (e.g. development of s-shaped and "comma-head" echoes, Fig. 4d-e). Additionally, throughout and following the merger process the supercell remained evident as a localized maximum in updraft helicity, while the squall line largely weakened north of the merger and evolved into a bow echo structure to the south of the merger (Fig. 5a).

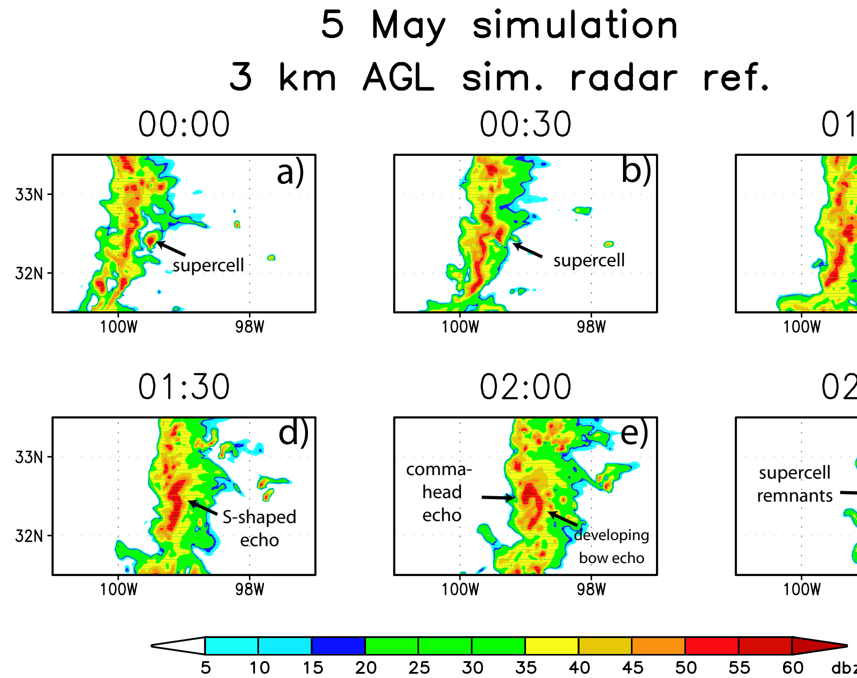


Figure 4: Simulated radar reflectivity at 3 km AGL for 5 May simulation at (a) 0000, (b) 0030, (c) 0100, (d) 0130, (e) 0200, and (f) 0230 UTC.

| | |
|---|---|
| Microphysics | Thompson double-moment |
| Boundary layer | Mellor-Yamada-Janic TKE |
| Land Surface | Noah |
| Surface Layer | Monin-Obukhov |
| Longwave radiation | RRTM |
| Shortwave radiation | Dudhia |

Table 1: Summary of physical parameterizations used in WRF simulations.

Ultimately the isolated supercell re-emerged west of the squall line as the bow echo accelerated toward the east, and eventually dissipated (Fig. 4f). While this behavior (the reemergence of an isolated supercell) was not observed in reality, the overall character of the merger and many of the simulated structures were qualitatively very similar to those observed in the actual case. This gives us confidence that the simulation captured many of the relevant processes that govern this merger process.

### *4.2 24 May 2008 Case*

An overview of the convective evolution observed during the squall line-supercell merger on 24 May 2008 is provided in figure 3e-h. The event consisted of two distinct supercells merging with an intense squall line that had developed along the dryline in western Kansas around 00 UTC on 24 May. The first of these mergers facilitated a break in the line, leading to the merger location becoming the north end of the squall line. The second merger occurred approximately an hour later, with the second storm also merging with the north end of the squall line. As was seen in the majority of our observed cases, structures related to the supercellular mode, including velocity couplets and inflow notches, remained evident in WSR-88D velocity and reflectivity data following the merger. A detailed analysis of the observed evolution and background environment associated with this case is included in French and Parker (2009).

To simulate the 24 May 2008 case, the WRF model was run over a domain centered on the central plains of the United States (Fig. 2a) from an initial time of 1200 UTC on 23 May 2008, approximately 12 hours before the event. Convection develops in the model around 2100 UTC in southwestern Kansas along the Oklahoma border (not shown), and several isolated supercell structures are present over this region between this time and 0000 UTC, qualitatively similar to what was observed in reality. The squall line began to develop in western Kansas around 0400 UTC, about 4 hours later than what was observed, however the approximate location and general structure of the line corresponds well with observations. By 0600 UTC, a single, large supercell had become dominant to the east of where the squall line was developing (Fig. 6a). Over time the supercell evolved from this large, high-precipitation organization to more of a classic supercell structure (Fig. 6a-c), and eventually merged with the squall line around 0900

UTC in central Kansas (Fig. 6d). Shortly after the merger, the updraft and vertical vorticity associated with supercell rapidly weakened, and it appeared to become absorbed into the squall line (e.g. Fig. 6e-f). This is evident in a time series of updraft helicity (Fig. 5b), which shows a rapid decrease and ultimate dissipation of the maximum associated with the supercell following the merger. While not an exact recreation of observations for 24 May, this simulation captures many of the salient features of that case, especially in terms of the isolated supercell merging with the northern end of the squall line, which is quite similar to the second merger event observed on this date.

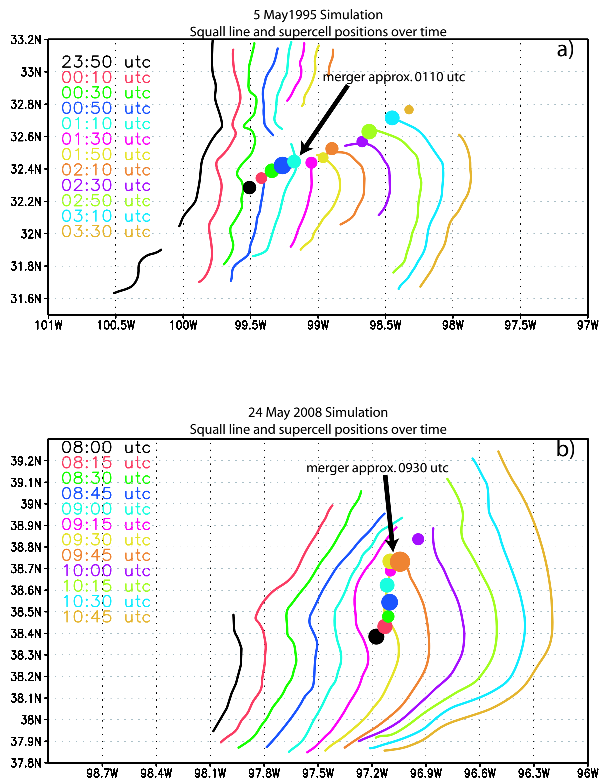


Figure 5: Isochrones of squall line position (lines) and supercell updraft location (dots) over time for (a) 5 May 1995 simulation and (b) 24 May 2008 simulation, color coded as per the key on the left side of the panels. Squall line isochrones correspond to the center of the region of gust front lifting greater than 1 ms at 1 km AGL. Supercell positions correspond to isolated maxima of updraft helicity greater than 25 $m^2s^{-2}$ associated with the supercell. Dot size roughly corresponds to the size of the 25 $m^2s^{-2}$ updraft helicity contour.

## 5. ANALYSIS

As outlined in the previous section, two simulations of squall line-supercell mergers have produced distinctly different results. In the 5 May simulation, the supercell was clearly sustained throughout the merger processes, and emerged as an isolated entity behind the squall line over an hour after the merger. Conversely, in the 24 May simulation, the supercell rapidly weakened following the merger and lost any defining supercell characteristics, becoming absorbed by the squall line. We will now examine the merger process in both of these simulations in more detail to determine what caused two different outcomes.

The merger in the 5 May simulation was preceded by a local weakening of the squall line, similar to what was observed in several actual cases as a break or weakening of the intense reflectivity in the convective region of the squall line. As the squall line neared the supercell, the outflow along the rear flank of the supercell created a pool of cold air that impeded the flow of conditionally unstable environmental air to the squall line's gust front (Fig. 7a). This cooler air locally weakened the temperature gradient along the gust front, leading to a rapid decline in low-level w and a general weakening of the squall line west of the supercell (Fig. 7b). As the storms merged, new low-level updraft "filled in" along a new gust front connecting the supercell and squall line (Fig. 7c). Thus, by the time the merger was complete, the supercell, rather than being overtaken by the squall line's cold pool, instead locally became the new leading edge of the squall line. This allowed high-$\theta_e$ and high storm-relative helicity (SRH) environmental air to continue to flow into the supercell and sustain both its updraft and mesocyclone.

Because it was never disrupted by the squall line's cold pool, the strong circulation and resultant low-pressure center associated with the supercell continued to draw environmental air into the storm, even as the squall line surged ahead to its south. Fig. 8a-b illustrates this as moist, hi-$\theta_e$ air continues to feed the supercell well after the merger, even as it moves rearward relative to the squall line. Thus, in the 5 May simulation, the supercell was sustained due to the combined effects of two key processes. First, outflow associated with the supercell locally weakened the squall line's gust front, effectively keeping this cold air from sweeping under the supercell and cutting off its source of sustaining high-$\theta_e$air. Second, because the supercell was not disrupted initially, it maintained a strong circulation, allowing it to continue to draw in environmental air, even as it moved rearward with respect to the squall line's gust front.

Several of these evolutionary details were also seen in the 24 May simulation, although the ultimate demise of the 24 May supercell demonstrates that the two cases were not identical. First, while perhaps not as dramatic as in the 5 May case, there

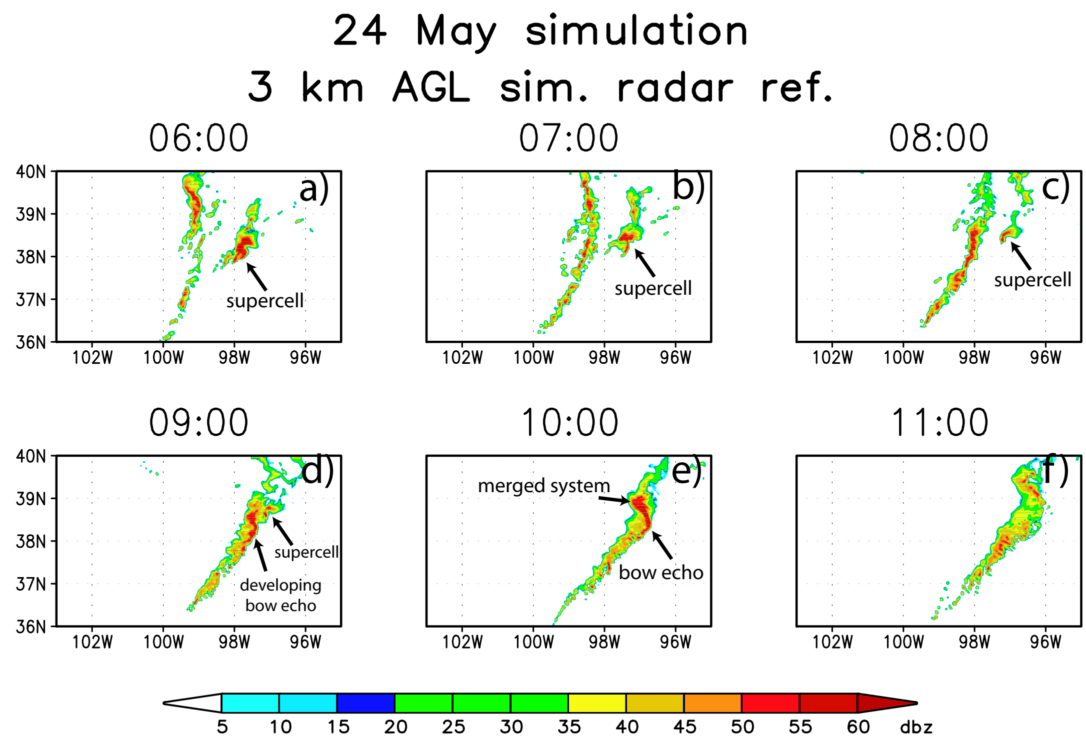


Figure 6: As in Fig. 4, but for 24 May simulation at (a) 0600, (b) 0700, (c) 0800, (d) 0900, (e) 1000, and (f) 1100 UTC.

is still some evidence that the gust front is locally slowed in the vicinity of the supercell in the 24 May simulation. An analysis of the gust front position leading up to merger time suggests a distinct westward lag towards the north end of the line, while further south the squall line begins to develop a bowing structure (heavy contour, Fig. 9a). Additionally, in the half hour immediately preceding the merger, a similar weakening of the low-level gust front updraft to what was observed in the 5 May simulation occurs (Fig 9b). As the supercell approaches the squall line, low level vertical motion along the gust front locally diminishes, and eventually disappears, as new updraft appears to develop and "fill in" between the gust front updraft to the south, and the supercell updraft. This evolution is quite similar to what was observed in the 5 May run. Finally, shortly after the merger is complete the merged system's cold pool strengthens south of the merger, with a concurrent intensification of bow-echo structure and low-level wind field, as was seen in the 5 May simulation (Fig 9c).

Despite the common evolutions seen in the two model runs, it is clear that there are different processes at work. One of the largest differences between the two runs is the lack of cold outflow associated with the 24 May supercell (e.g. Fig. 9), likely owing to its evolution toward more of a classic supercell structure, as opposed to the HP structure in the 5 May simulation. Thus, a different mechanism must be responsible for the observed behavior in this simulation. One feature that stands out is a persistent warm anomaly around 1 km AGL that at times covers the entire area between the western flank of the supercell and the squall line (Fig. 11a-c). This localized warm pocket appears to be associated with subsidence, which also drives substantial drying in the same region, leading to a considerable decrease in CAPE (not shown). This decrease in CAPE would help explain the apparent weakening of the gust front updraft. What is less clear is what process is driving the subsidence that causes this local decline in CAPE. While it stands to reason that the subsiding motion near the rear flank of the supercell is associated with the rear flank downdraft, given the comparatively large areal extent of the warming, it seems unlikely that this is the sole process at work. Seeing as this warming at times spans the entire region between the squall line and supercell, and that it first develops around the same time that the squall line starts to intensify and approach the supercell, we speculate that this heating may be due to some interaction between the two systems. One possible explanation is a localized superposition of convectively-generated waves of subsidence (i.e. the n=1 wave mode discussed by Nicholls et al. (1991) and Mapes (1993)) associated with both convective modes. Further analysis to this end is ongoing, and we hope to be able to provide a more definitive answer in a future publication.

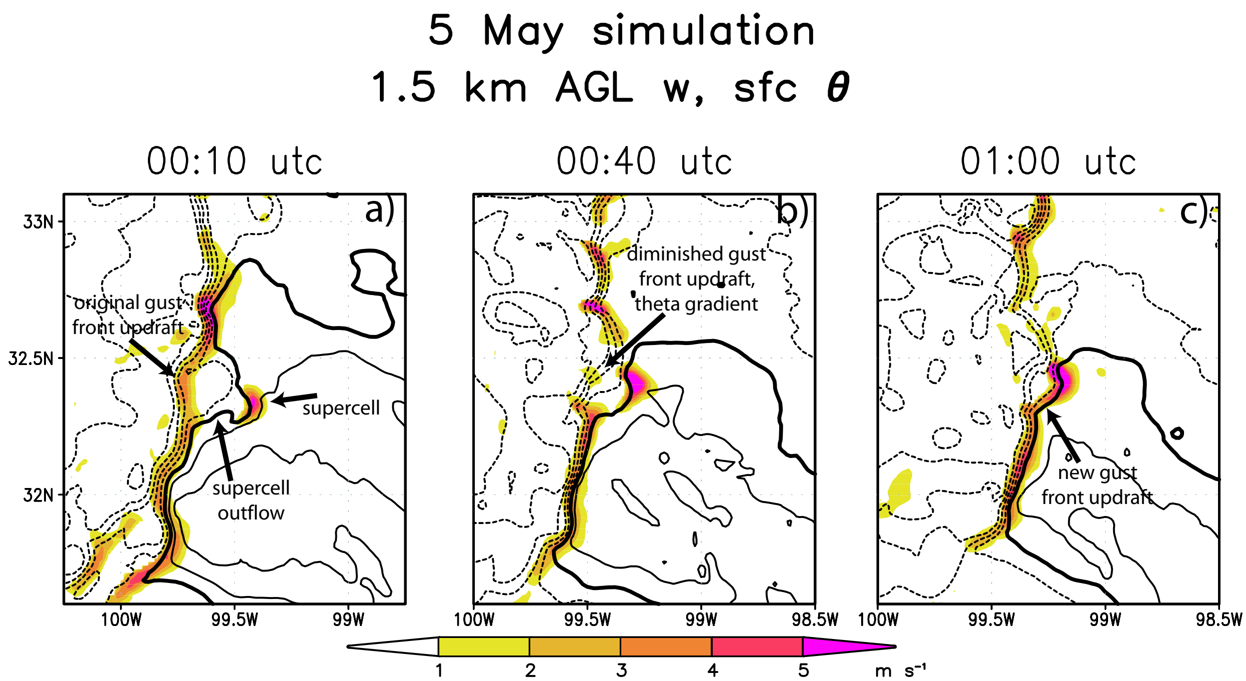


Figure 7: Time series of 1.5 km AGL w (m s$^{-1}$, shaded as shown) and surface potential temperature (K, contoured every 1 K, values greater than 300 K (heavy contour) are solid, less than 300 K dashed) at (a) 0010, (b) 0040 and (c) 0100 UTC .

The other key difference between the simulations is that the supercell structure in the 24 May simulation does not survive for very long following the merger, likely due to the removal of high-$\theta_e$, high SRH environmental inflow shortly after thereafter. Immediately following the merger (Fig. 8c) the supercell remains evident as an isolated maximum of updraft helicity and is being fed by a thin ribbon of warm environmental air that extends to its south and southeast. An hour later (Fig. 8d) this ribbon of inflow has disappeared along with the isolated core of strong updraft helicity. This is a stark contrast to what is observed an hour after the merger in the 5 May simulation (Fig. 8b). It is not clear whether the weakening of the supercell was caused by the merger itself, or if it was due to the storm's movement into increasingly stable air north of a nearby low-level thermal boundary (evident in Figs. 9a-c). Given some of the similarities between the simulations up to and immediately after the merger, we speculate that the presence of the boundary may have been critical to the supercell's demise. In both simulations, the squall line's cold pool intensifies south of the merger point (e.g. Fig. 8b, d) and continues to move east with the supercell moving rearward in a gust front-relative sense (e.g. Fig. 5). In the 5 May case, a region of high-$\theta_e$ environmental air is present east of the merger location, and the supercell is able to continue to ingest surface-based inflow along the northern edge of the bowing line segment (Fig. 8b). However, in the 24 May simulation, the airmass to the east of the merged system is considerably cooler and more stable owing to the thermal boundary. As a result, the supercell's only source of undisturbed surface-based air is from the south (Fig. 8c), and once the cold pool intensifies and moves eastward post-merger, the supercell is effectively cut off from this surface-based inflow (Fig. 8d). The result is an ultimate weakening of the supercell as the entire northern end of the merged system moves into the more stable airmass and becomes elevated. We speculate that in the absence of the low-level boundary, the supercell in the 24 May simulation would have continued to ingest surface-based inflow, and may have instead evolved in a manner similar to the 5 May simulation, which is more consistent with many of our observed cases.

## 6. CONCLUSIONS AND FUTURE WORK

WRF simulations were performed for two cases of squall line-supercell mergers, providing insight into several key processes that appear to be important for the merger process. One simulation captured the maintenance of supercell structures while the other produced a cessation of supercell features. A few general conclusions can be drawn. First, a key part of the process preceding the actual merger is that the presence of the supercell appears to facilitate a localized weakening of the squall line and its associated gust front, apparently through the interruption of the flow of high-CAPE, low CIN parcels into the gust front updraft. In the 5 May simulation this was accomplished by the cold surface outflow associated

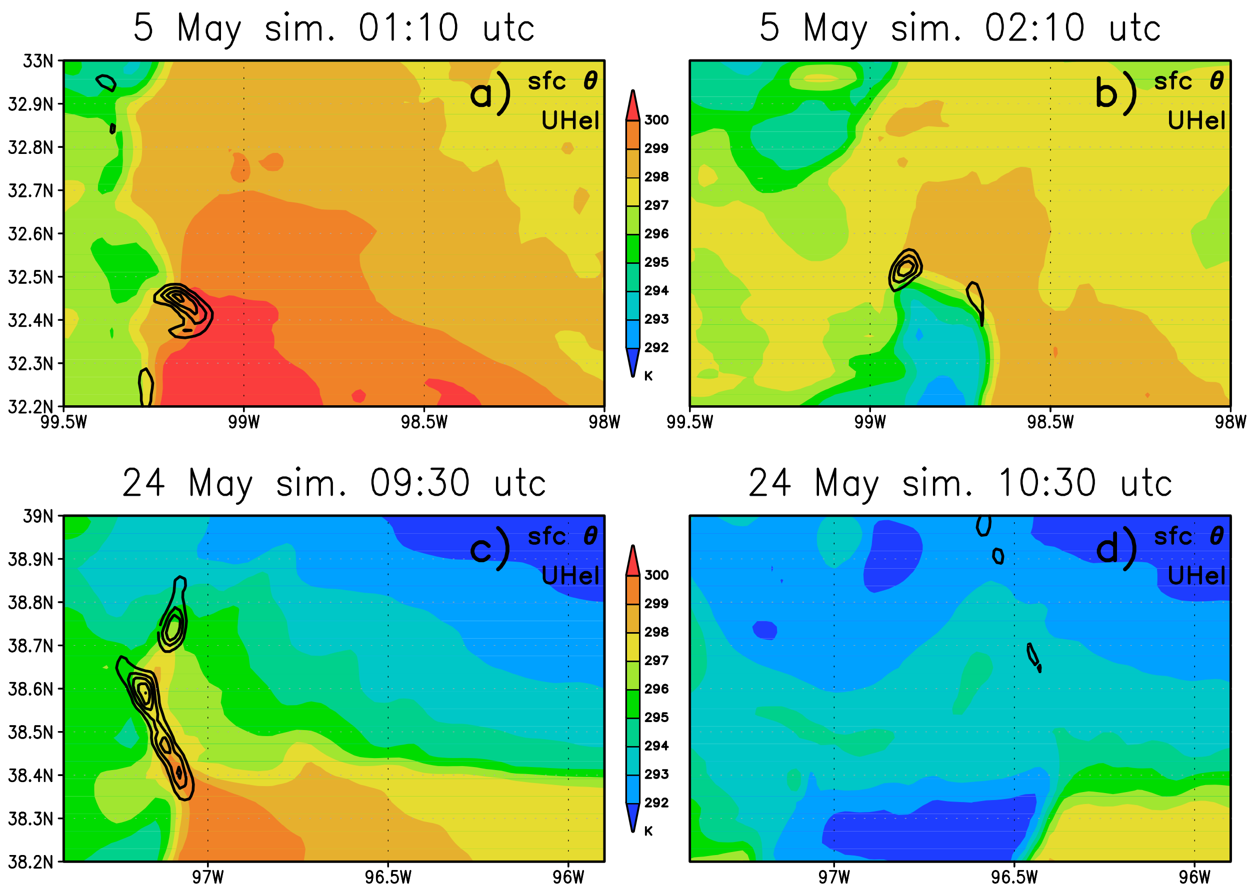


Figure 8: Surface potential temperature (shaded as shown) and updraft helicity (positive values contoured every 25 $m^2s^{-2}$) for 5 May simulation at (a) 0110 UTC and (b) 0210 UTC and 24 May simulation at (c) 0930 UTC and (d) 1030 UTC. Note that the color bar differs for the top and bottom panels.

with the rear flank of the supercell effectively cutting of the flow of environmental air to the squall line. In the 24 May case a region of strong subsidence between the supercell and squall line lead to warming and drying of the low-level air, resulting in a significant reduction in CAPE just ahead of the gust front. In the 5 May case, this weakening of the squall line appeared to keep the cold outflow associated with the squall line from overtaking the supercell and cutting off its inflow.

The second general conclusion is that the continued maintenance of supercell structures (i.e. strong mid-level updraft and vorticity maxima) following the merger appears to be controlled by the ability of the supercell to continue ingesting surface-based conditionally unstable air parcels after the merger. In the 5 May simulation, the embedded supercell continued to draw environmental air into its updraft well after the merger, even as the squall line surged eastward and ahead of it. As a result the supercell structure was maintained, to the point of re-emerging west of the squall line as an isolated storm over an hour after the merger occurred. Conversely, in the 24 May simulation, the narrow ribbon of inflowing environmental air was cut off from the supercell shortly after the merger occurred, and the supercell rapidly weakened in terms of updraft intensity and vertical vorticity. It remains unclear whether this was due to the supercell being undercut by the squall line's outflow, or whether it was due to the merged system moving north across a thermal boundary into a cooler, more stable airmass and becoming elevated. Either way, this evolution illustrates that uninterrupted environmental inflow appears key to supercell longevity in these cases.

Additional work remains ongoing with this project. Of primary importance is running additional simulations of these and several other cases using smaller horizontal grid spacings of 1 km and 333 m in order to more effectively resolve convective scale processes. Using these higher resolution simulations, our goal is to more quantitatively ex-

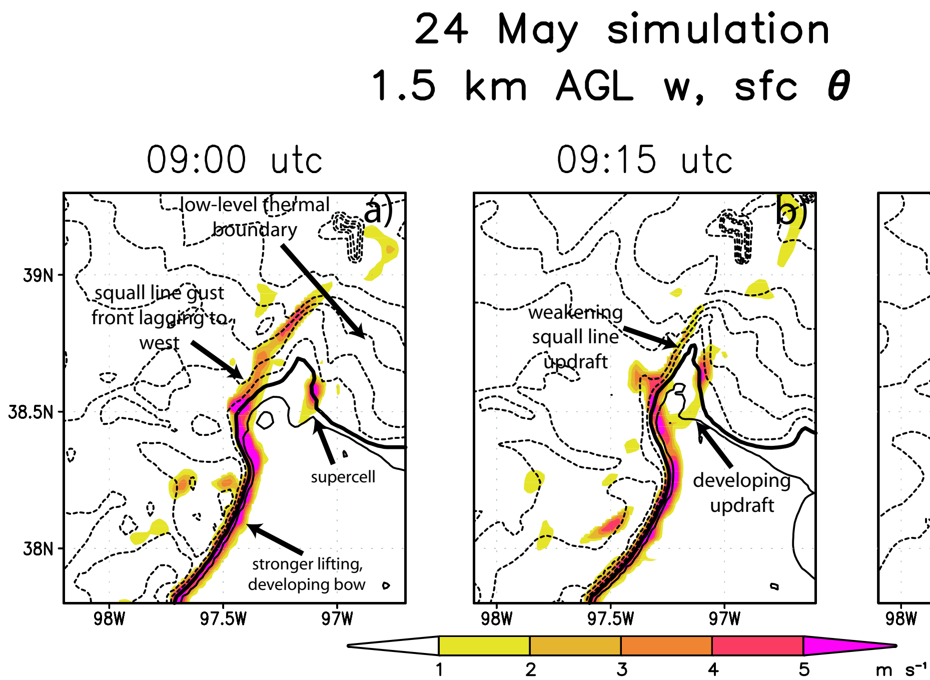


Figure 9: As in Fig. 7, but for 24 May simulation, at (a) 0900 , (b) 0915 , and (c) 0930 UTC, with values less than 298 K (heavy contour) dashed and greater than 298 K solid.

plain the processes outlined in this paper, while also shedding more light on some remaining questions, such as the processes responsible for the localized warming observed in the 24 May simulation, and the precise role this plays in the squall line-supercell merger process. Additionally, we are also investigating ways in which these two convective modes may interact prior to merging, or in cases where the storms are both present but do not actually merge. By doing so, we hope to construct a more complete picture of the role that interactions between these storms play throughout the duration of these types of multi-convective mode events.

*Acknowledgments*

The authors would like to thank the members of the Convective Storms Group at NC State University: Casey Letkewicz, Matt Morin and Johannes Dahl for their thoughtful discussion and assistance in the course of this work. This work is funded by NSF grants ATM-0552154 and ATM-0758509.

References

Bunkers, M. J., M. R. Hjelmfelt, and P. L. Smith, 2006: An observational examination of long-lived supercells. Part I: Characteristics, evolution, and demise. *Wea. Forecasting*, **21**, 673–688.

Calianese, E. J., J. K. Jordan, E. B. Curran, A. R. Moller, and G. Woodall, 2002, The Mayfest high-precipitation supercell of 5 May 1995-a case study. Preprints, *21st Conference on Severe Local Storms*, San Antonio, TX, Amer. Meteor. Soc.

French, A. J. and M. D. Parker, 2008: The initiation and evolution of multiple modes of convection within a meso-alpha scale region. *Wea. Forecasting*, **23**, 1221–1252.

French, A. J. and M. D. Parker, 2009, Mergers between isolated supercells and quasi-linear convective systems: A preliminary study. Preprints, *13th Conf. Mesoscale Processes*, Salt Lake City, UT, Amer. Meteor. Soc.

Goodman, S. J. and K. R. Knupp, 1993, Tornadogenesis via squall line and supercell interaction: The November 15, 1989, Huntsville, Alabama, tornado. *The Tornado: Its Structure, Dynamics, Prediction, and Hazards.* No. 79, Amer. Geophys. Union.

Knupp, K. R., S. Paech, and S. Goodman, 2003: Variations in cloud-to-ground lightning characteristics among three adjacent tornadic supercell storms over the tennessee valley region. *Mon. Wea. Rev.*, **131**, 172–188.

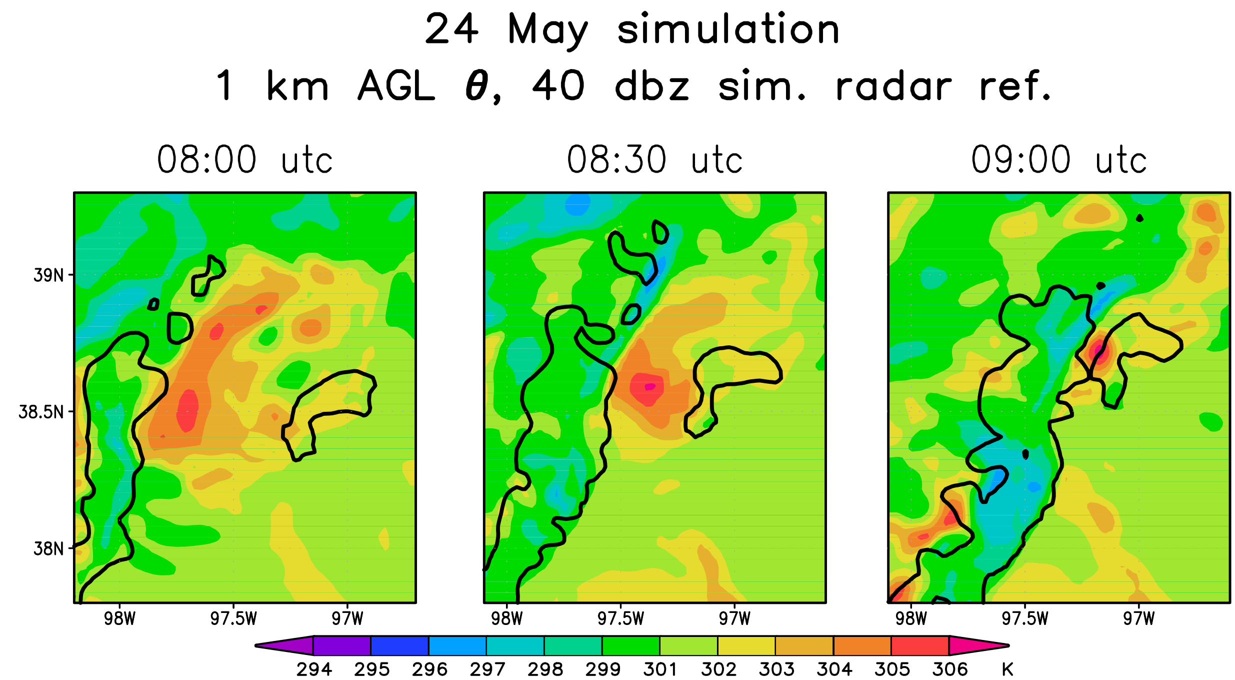


Figure 10: Potential temperature (shaded, K) at 1 km AGL and 40 dbz simulated radar reflectivity contour at (a) 0800 UTC, (b) 0830 UTC and (c) 0900 UTC for the 24 May simulation.


Lindsey, D. T. and M. J. Bunkers, 2005: Observations of a severe, left-moving supercell on 4 May 2003. *Wea. Forecasting*, **20**, 15–22.

Mapes, B. E., 1993: Gregarious tropical convection. *J. Atmos. Sci.*, **50**, 2026–2037.

Nicholls, M. E., R. A. Pielke, and W. R. Cotton, 1991: Thermally forced gravity waves in an atmosphere at rest. *J. Atmos. Sci.*, **48**, 1869–1884.

Sabones, M., E. M. Agee, and M. Akridge, 1996, The Pulaski county and West Lafayette, Indiana tornadoes, 26-27 April 1994: A case of supercell (mesocyclone) and squall line bow-echo interaction. Preprints, *18th Conf. Severe Local Storms*, San Francisco, CA, Amer. Meteor. Soc.

Wolf, P. L., 1998: WSR-88D radar depiction of supercell-bow echo interaction: Unexpected evolution of a large, tornadic "comma-shaped" supercell over eastern Oklahoma. *Wea. Forecasting*, **13**, 492–504.

Wolf, R., R. Przybylinski, and P. Berg, 1996, Observations of a merging bowing segment and supercell. Preprints, *18th Conf. Severe Local Storms*, San Francisco, CA, Amer. Meteor. Soc.